Articles in PresS. Am J Physiol Regul Integr Comp Physiol (March 8, 2017). doi:10.1152/ajpregu.00530.2016

R-00530-2016R1

Aortic depressor nerve stimulation does not impede dynamic characteristics of the carotid sinus baroreflex in normotensive or spontaneously hypertensive rats

Authors: Toru Kawada*, Michael J Turner*, Shuji Shimizu, Masafumi Fukumitsu, Atsunori Kamiya, Masaru Sugimachi

*These authors contributed equally to this study.

Affiliations: Department of Cardiovascular Dynamics, National Cerebral and Cardiovascular Center, Osaka 565-8565, Japan

Short title: ADN stimulation and carotid sinus baroreflex

Corresponding author:

Toru Kawada, MD, PhD

Department of Cardiovascular Dynamics, National Cerebral and Cardiovascular Center, 5-7-1 Fujishirodai, Suita-shi, Osaka 565-8565, Japan

Tel: +81-6-6833-5012 (ext. 2427)

Fax: +81-6-6835-5403

e-mail: torukawa@ri.ncvc.go.jp

Abstract

Recent clinical trials in patients with drug-resistant hypertension indicate that electrical activation of the carotid sinus baroreflex can reduce arterial pressure (AP) for more than a year. To examine whether the electrical stimulation from one baroreflex system impedes normal short-term AP regulation via another unstimulated baroreflex system, we electrically stimulated the left aortic depressor nerve (ADN) while estimating the dynamic characteristics of the carotid sinus baroreflex in anesthetized normotensive Wistar–Kyoto (WKY, n = 8) rats and spontaneously hypertensive rats (SHR, n = 7). Isolated carotid sinus regions were perturbed for 20 min using a Gaussian white noise signal with a mean of 120 mmHg for WKY and 160 mmHg for SHR. Tonic ADN stimulation (2 Hz, 10 V, 0.1-ms pulse width) decreased mean sympathetic nerve activity (73.4 ± 14.0 vs. 51.6 ± 11.3 arbitrary units in WKY, P = 0.012; and 248.7 ± 33.9 vs. 181.1 ± 16.6 arbitrary units in SHR, P = 0.018) and mean AP (90.8 ± 6.6 vs. 81.2 ± 5.4 mmHg in WKY, P=0.004; and 128.6 ± 9.8 vs. 114.7 ± 10.3 mmHg in SHR, P = 0.009). The slope of dynamic gain in the neural arc transfer function from carotid sinus pressure to sympathetic nerve activity was not different between trials with and without the ADN stimulation (12.55 ± 0.93 vs. 13.03 ± 1.28 dB/decade in WKY, P = 0.542; and 17.37 ± 1.01 vs. 17.47 ± 1.64 dB/decade in SHR, P = 0.946). These results indicate that the tonic ADN stimulation does not significantly modify the dynamic characteristics of the carotid sinus baroreflex.

Keywords: transfer function, Gaussian white noise, sympathetic nerve activity, arterial pressure.

Introduction

The arterial baroreflex system provides an important negative feedback mechanism to stabilize arterial pressure (AP) against pressure disturbance such as that occurs during postural changes. The significance of the arterial baroreflex in the long-term AP control has been somewhat underestimated partly because the arterial baroreflex shows resetting to prevailing AP levels [6]. Sinoaortic baroreceptor denervation increases the variation of AP but does not induce a sustained increase in mean AP beyond a few days [7], suggesting the importance of the arterial baroreflex in the short-term stabilization of AP rather than the long-term determination of mean AP. Nevertheless, recent findings indicate that lowering carotid sinus pulsatile pressure can increase AP for a longer period than ever thought before [25] and electrical baroreflex activation can induce a sustained reduction in AP for three weeks [17]. Based on these findings, baroreflex activation therapy, which dates back to the 1960s as a method for pain relief from angina pectoris [5], has received renewed interest as a potential treatment of drug-resistant hypertension [2, 29]. During carotid sinus baroreflex activation therapy, carotid sinus baroreceptors are electrically stimulated whereas the aortic baroreceptors sense information on native AP changes. While carotid sinus stimulation (CSS) does not impede but rather restores spontaneous baroreflex control in a canine model of obesity-induced hypertension [11], whether CSS impedes dynamic characteristics of the unstimulated arterial baroreflex remains unknown.

The arterial baroreflex system may be analyzed by dividing it into two principal subsystems. One is the neural arc, which quantifies the relationship

between baroreceptor input pressure and efferent SNA. The other is the peripheral arc, which quantifies the relationship between efferent SNA and AP. We have estimated dynamic characteristics of the neural and peripheral arcs by perturbing isolated carotid sinus baroreceptor regions with a Gaussian white noise (GWN) pressure input [18]. The neural arc reveals derivative characteristics in the frequency range from 0.01 to 1 Hz in rabbits and rats [10, 12, 14], which compensate for low-pass characteristics of the peripheral arc to achieve quick and stable AP regulation mediated by the carotid sinus baroreflex. Given the presence of interactions between sinoaortic baroreflexes depending on the size of input signals [31], we hypothesized that aortic depressor nerve (ADN) stimulation may impede dynamic characteristics of the carotid sinus baroreflex. We are aware that the carotid sinus baroreflex is electrically activated and the aortic baroreflex receives native pressure inputs in clinical CSS. However, we reversed the situation because of the technical difficulty in selectively stimulating short carotid sinus nerves in rats and assume that electrical ADN stimulation can mimic the situation of clinical CSS.

The ADN of rats contains myelinated axons (A-fiber, approximately 10–20%) and unmyelinated axons (C-fiber, approximately 80–90%) [1,9]. Low-voltage (3 V), high-frequency (>10 Hz) stimulation preferentially activates the A-fiber pathway whereas high-voltage (18 V), low-frequency (<10 Hz) stimulation preferentially activates the C-fiber pathway [8]. As the C-fiber pathway plays a dominant role in the sustained inhibitions of SNA and AP [26, 28], the C-fiber pathway likely contributes to the CSS-mediated antihypertensive effect. Hence, we used high-voltage, low-frequency stimulation to examine the

effect of the ADN stimulation on the dynamic characteristics of the carotid sinus baroreflex. The experiment was performed on anesthetized normotensive Wistar–Kyoto (WKY) rats and spontaneously hypertensive rats (SHR).

Methods

Animals were cared for in strict accordance with the National Institutes of Health (NIH) Guide for the Care and Use of Laboratory Animals, and with the Guiding Principles for the Care and Use of Animals in the Field of Physiological Sciences approved by the Physiological Society of Japan. All experimental protocols were reviewed and approved by the Animal Subjects Committee at the National Cerebral and Cardiovascular Center.

Surgical preparation

Male WKY (n = 8) and SHR (n = 7) aged 12–14 weeks were used in the present study. Each rat was anesthetized with an intraperitoneal injection (2 ml/kg) of a mixture of urethane (250 mg/ml) and α-chloralose (40 mg/ml). Artificial ventilation with oxygen-supplemented room air was performed via a tracheal intubation. A venous catheter was inserted into the right femoral vein for the continuous administration of 18-fold diluted solution of the above anesthetic mixture (2–3 $ml \cdot kg^{-1} \cdot h^{-1}$). An arterial catheter was inserted into the right femoral artery to measure AP.

A postganglionic branch of the left splanchnic sympathetic nerve was approached retroperitoneally. A pair of stainless steel wire electrodes (AS633, Cooner Wire, CA, USA) was attached to the nerve using silicone glue (Kwik-Sil, World Precision Instruments, FL, USA) to record SNA. The pre-amplified nerve

signal was band-pass filtered between 150 and 1,000 Hz, and then full-wave rectified and low-pass filtered with a cut-off frequency of 30 Hz.

The carotid sinus regions were isolated from the systemic circulation bilaterally [21, 23], and were filled with warmed Ringer solution through catheters inserted into the common carotid arteries. The other ends of the catheters were connected to a servo-controlled piston pump to impose pressure inputs. Bilateral vagal and aortic depressor nerves were sectioned at the neck to avoid reflexes from the cardiopulmonary region and aortic arch. A pair of stainless steel wire electrodes (AS633) was attached to the sectioned left ADN for afferent fiber stimulation. The electrodes and the nerve were insulated by silicone glue (Kwik Sil). The electrical stimulation of the ADN was performed through an isolator from an electric stimulator (SEN-7203, Nihon Kohden, Japan).

Protocols

An anesthetized in situ preparation of the carotid bifurcation was used. After the completion of the surgical preparation, a stabilization period of more than 30 min was allowed before the data acquisition. To estimate open-loop dynamic characteristics of the carotid sinus baroreflex, carotid sinus pressure (CSP) was perturbed with a GWN signal with a standard deviation of 20 mmHg for 20 min. The mean level of GWN was set at 120 mmHg for WKY and 160 mmHg for SHR according to a previous study [13]. The switching interval of the signal was set at 500 ms, which allowed estimation of the transfer function up to approximately 1 Hz. The CSP perturbation trial was performed with or without a tonic ADN stimulation. The stimulation voltage was set at 10 V, which is

sufficiently high to activate both A- and C-fiber axons. However, the stimulation frequency was set at 2 Hz to induce primarily the C-fiber baroreflex [8]. The pulse width was set at 0.1 ms. The order of the trials with or without the ADN stimulation was randomized among animals. At the end of the experiment, a ganglionic blocker hexamethonium bromide (60 mg/kg) was administered intravenously to determine the noise level of SNA.

Data analysis

Data were stored at 200 Hz through a 16-bit analog-to-digital converter (ADA16-8/2(CB)L, Contec, Japan) using a custom-made software. Data were analyzed beginning at 5 min after the onset of the CSP perturbation. To estimate the neural arc transfer function, CSP and SNA were treated as the input and the output of the system, respectively. To estimate the peripheral arc transfer function, SNA and AP were the input and the output of the system, respectively. To estimate the total reflex arc transfer function, CSP and AP were the input and the output of the system, respectively.

The input–output data pairs were resampled at 10 Hz, and were divided into 12 half-overlapping segments of 1,024 data points each. In each segment, after removing the linear trend and applying a Hanning window, frequency spectra of the input [$S_X(f)$] and the output [$S_Y(f)$] were calculated via the fast Fourier transform. Ensemble averages of the input power spectra [$S_{XX}(f)$], the output power spectra [$S_{YY}(f)$], and the cross spectra [$S_{YX}(f)$] were calculated over the 12 segments. Finally, the transfer function [$H(f)$] was estimated from the following equation [4].

$$H(f) = \frac{S_{YX}(f)}{S_{XX}(f)} \quad (1)$$

The magnitude-squared coherence function [*Coh*(*f*)] was also calculated from the following equation [4].

$$Coh(f) = \frac{|S_{YX}(f)|^2}{S_{XX}(f)S_{YY}(f)} \quad (2)$$

The coherence function, which ranges from zero to unity, is a measure of linear dependence between the input and the output in the frequency domain. To help intuitive understanding of the estimated dynamic characteristics, the step response corresponding to the transfer function was obtained from the time integral of the inverse Fourier transform of the estimated transfer function.

SNA was normalized in each animal and presented in arbitrary units (a.u.) because the absolute amplitude of SNA varied among animals depending on the recording conditions. The noise level measured after the ganglionic blockade was subtracted, and then a normalization factor of SNA was determined so that the mean dynamic gain in frequencies below 0.03 Hz became unity in the neural arc transfer function obtained in the trial without the ADN stimulation. The same normalization factor was applied to the neural arc transfer function obtained in the trial with the ADN stimulation. An inverse of the normalization factor was applied to the peripheral arc transfer functions.

Statistical analysis

All data are presented as mean and SE values. Several parameters were arbitrary selected to compare the transfer functions and step responses as follows. For the neural arc, the dynamic gain values at 0.01, 0.1, and 1 Hz ($G_{0.01}$, $G_{0.1}$, and G_1) were used to represent the transfer function. The slope of dynamic

gain (G_{slope}) was estimated by linear regression between the logarithm of frequency and the logarithm of dynamic gain in the frequency range from 0.1 to 1 Hz, and was expressed in decibel (dB) per decade. For the step response of the neural arc, the negative peak response (S_{peak}), time to the negative peak (T_{peak}), and the step response at 10 s (S_{10}) were calculated. For the peripheral arc and the total reflex arc, the dynamic gain values at 0.01, 0.1, and 0.5 Hz ($G_{0.01}$, $G_{0.1}$, and $G_{0.5}$) were used to represent the transfer function. G_{slope} was estimated in the frequency range from 0.05 to 0.5 Hz. For the step responses of the peripheral arc and the total reflex arc, the initial slope (S_{slope}) and the steady-state response at 50 s (S_{50}) were calculated. The speed of the step response was assessed by S_{slope}/S_{50}. The comparison was performed using a paired-t test between trials with and without the ADN stimulation separately for the WKY and SHR groups because the comparison of dynamic baroreflex characteristics between WKY and SHR, which was done in a previous study [13], was outside the primary purpose of the present study.

To help consider possible plasticity of the arterial baroreflex, an additional analysis was performed. Data during the 20-min GWN input were divided into 4 consecutive 5-min bins (the first bin was not used for the transfer function analysis described above), and mean SNA and AP in each bin were calculated. For each bin, differences in mean AP and mean SNA between the trials with and without the ADN stimulation were designated as ΔAP and ΔSNA, respectively. Changes in mean AP and SNA across the 4 bins in the trial without the ADN stimulation were examined using one-way repeated-measures analysis of variance (ANOVA) followed by the Dunnett's test against the values in bin #1.

Likewise, changes in ΔAP and ΔSNA were examined against the values in bin #1. In all the statistical analyses, the difference was considered significant at $P < 0.05$.

Results

Dynamic characteristics of the carotid sinus baroreflex in the WKY group

Figure 1 depicts typical time series obtained from one WKY rat. CSP was changed dynamically according to a GWN signal with a mean of 120 mmHg. The sequence of GWN was different between animals but identical in each animal for ease of paired comparison. In the AP plots, the gray and black lines indicate 200-Hz sampled signals and 2-s moving averaged signals, respectively. In the SNA plots, the gray and black lines indicate 10-Hz resampled signals and 2-s moving averaged signals, respectively. Compared with the trial without the ADN stimulation (left panels), the ADN stimulation reduced the mean levels of AP and SNA and attenuated their variations (middle panels). Cessation of the external control reduced CSP to approximately 80 mmHg in this animal (right panels), which resulted in an increase in AP compared with AP values during the CSP perturbation trials. The intravenous administration of hexamethonium bromide (C6) reduced SNA to the noise level, which was zero a.u. by definition. Pooled data from the WKY group indicated that the trial with the ADN stimulation resulted in lower mean AP (90.8 ± 6.6 vs. 81.2 ± 5.4 mmHg, $P = 0.004$) and lower mean SNA (73.4 ± 14.0 to 51.6 ± 11.3 a.u., $P = 0.012$) for the period of the transfer function analysis compared with the trial without the ADN stimulation.

Figure 2 illustrates transfer functions and step responses obtained from

the trial with (black lines) or without (gray lines) the ADN stimulation averaged for the WKY group. In the neural arc transfer function (left panels), dynamic gain increased with increasing frequency, which is referred to as derivative characteristics. The phase approached –π radians at the lowest frequency, reflecting the negative feedback operation via the vasomotor center. Coherence was approximately 0.5 at the lowest frequency and increased slightly between 0.1 and 1 Hz. The dynamic gain was slightly lower during the ADN stimulation, with significant lower values in $G_{0.1}$ and G_1 (Table 1). The derivative characteristics were, however, maintained during the ADN stimulation, as supported by no significant change in G_{slope}. The step response of the neural arc showed a negative peak. While S_{peak} was attenuated during the ADN stimulation, T_{peak} did not change significantly (Table 1).

In the peripheral arc transfer function of the WKY group (Fig. 2, middle), dynamic gain decreased with increasing frequency above approximately 0.04 Hz, which is referred to as low-pass characteristics. The phase approached zero radians at the lowest frequency, reflecting the fact that an increase in SNA increases AP at the steady-state response. Coherence was above 0.6 in the frequency range up to approximately 0.6 Hz. The peripheral arc transfer function and corresponding step response did not differ between trials with and without the ADN stimulation, and there were no significant changes in the parameter values (Table 1).

In the transfer function of the total reflex arc obtained in the WKY group (Fig. 2, right), dynamic gain decreased with increasing frequency above approximately 0.04 Hz. The phase approached –π radians at the lowest

frequency, indicating the fact that an increase in CSP decreases AP at the steady-state response. Coherence was approximately 0.5 in the frequency range up to approximately 0.6 Hz. The dynamic gain was slightly lower during the ADN stimulation, with significant lower values in $G_{0.01}$ and $G_{0.1}$ (Table 1). The low-pass characteristics hardly changed during the ADN stimulation, as supported by no significant change in G_{slope}. In the step response of the peripheral arc, S_{slope} and S_{50} were significantly less negative during the trial with the ADN stimulation than without. The speed of the AP response, as assessed by S_{slope}/S_{50}, however, did not differ between trials with and without the ADN stimulation (Table 1).

Dynamic characteristics of the carotid sinus baroreflex in the SHR group

Figure 3 depicts typical time series obtained from one SHR. CSP was changed dynamically according to a GWN signal with a mean of 160 mmHg. Compared to the trial without the ADN stimulation (left panels), the ADN stimulation reduced the mean levels of AP and SNA (middle panels). The reduction of CSP to 60 mmHg at the end of the experiment (right panels) resulted in a significant increase in AP compared with AP values during the CSP perturbation trials. The intravenous administration of hexamethonium bromide (C6) reduced SNA to the noise level. Pooled data from the SHR group indicated that the trial with the ADN stimulation showed lower mean AP (128.6 ± 9.8 vs. 114.7 ± 10.3 mmHg, P = 0.009) and lower mean SNA (248.7 ± 33.9 to 181.1 ± 16.6 a.u., P = 0.018) than the trial without the ADN stimulation when compared for the period of the transfer function analysis.

Figure 4 illustrates transfer functions and step responses obtained from

the trial with (black lines) or without (gray lines) the ADN stimulation averaged for the SHR group. The neural arc transfer function revealed derivative characteristics (left panels). While the mean gain plot showed a tendency of downward shift during the ADN stimulation, changes in the gain values at selected frequencies were not statistically significant possibly due to the large variation of data (Table 2). There were no significant differences in the parameter values of the neural arc step response between the trials with and without the ADN stimulation. The peripheral arc transfer function revealed low-pass characteristics (middle panels). None of the parameters of the peripheral arc transfer function or the step response differed between the trials with and without the ADN stimulation (Table 2). The transfer function of the total reflex arc revealed a decreased gain with increasing frequency (right panels). The dynamic gain showed large variations across frequencies and among animals. Although the mean step response tended to be attenuated, there was no statistically significant change in S_{50} (Table 2). S_{slope} was significantly less negative during the ADN stimulation, but S_{slope}/S_{50} did not change significantly between trials with and without the ADN stimulation.

Mean AP and SNA calculated for 4 consecutive 5-min bins during the GWN input are shown in Table 3. In WKY, the mean AP in the trial without the ADN stimulation did not change significantly among the 4 bins. While the ΔAP seemed less negative at bin #3 than at bin #1, the difference was not statistically significant, possibly because time-dependent changes were not consistent among animals. The mean SNA was significantly higher at bin #4 than at bin #1. The ΔSNA did not differ significantly among the 4 bins. In SHR, the mean AP in

the trial without the ADN stimulation did not change significantly among the 4 bins. The ΔAP was less negative at bin #4 than at bin #1. The mean SNA was significantly higher at bins #3 and #4 than at bin #1. The ΔSNA did not differ significantly among the 4 bins.

Discussion

The present study examined the effect of tonic C-fiber stimulation of the ADN on the dynamic characteristics of the carotid sinus baroreflex. The major finding is that despite the significant hypotensive effect, the ADN stimulation hardly impedes the dynamic characteristics of the carotid sinus baroreflex in either WKY or SHR.

Effects of ADN stimulation on dynamic characteristics of the carotid sinus baroreflex

The peripheral arc transfer function from SNA to AP was not changed significantly by the ADN stimulation in WKY (Fig. 2, middle) or SHR (Fig. 4, middle), despite the significant reductions of mean SNA and mean AP. The results are in line with a previous study that examined the operating-point dependence of the dynamic baroreflex characteristics, in which an increase in mean CSP did not significantly affect the peripheral arc transfer function regardless of the reductions of mean SNA and mean AP [15]. A possible reason for the relative insensitivity of the peripheral arc transfer function to the operating point is an approximately linear static input–output relationship between SNA and AP in WKY [39] and SHR [20]. As long as the operating point is within the linear input–output range, a difference in the operating point may not

significantly affect the peripheral arc transfer function. Hence, changes in the dynamic characteristics of the total reflex arc, if any, are mainly attributable to changes in the dynamic characteristics of the neural arc in the present study.

In WKY, the ADN stimulation slightly but significantly attenuated the dynamic gain of the neural arc, which was also reflected in the reduction of the dynamic gain of the total reflex arc. In contrast to the approximately linear relationship of the peripheral arc, the static input–output relationship of the neural arc reveals sigmoidal nonlinearity between CSP and SNA [12, 14, 30]. In the present study, the mean CSP was set at 120 mmHg, which is close to the midpoint or the steepest portion of the sigmoidal nonlinearity in WKY. Hence, the dynamic gain of the neural arc is expected to be near maximum as far as the mean CSP is concerned. However, the standard deviation of the GWN was set at 20 mmHg, which means that CSP exceeded 150 mmHg (mean + 1.5 standard deviation) in 6.7% of the time duration. Owing to the derivative characteristics of the neural arc, these high CSP inputs silenced SNA even without the ADN stimulation (Fig. 1, left). Although the ADN stimulation cannot affect the afferent signal from the carotid sinus baroreceptors directly, it reduced the mean SNA and increased the chance of silencing SNA (Fig. 1, middle). As the signal through the neural arc is truncated during the silencing of SNA, the dynamic gain of the neural arc may be attenuated during the ADN stimulation. The results may indicate an occlusive summation or an inhibitory interaction between the carotid sinus and aortic baroreflex central pathways during high CSP inputs. The results, however, would not conflict with a previous study indicating that the summation of sinoaortic baroreflexes could be regarded as simple additive when the CSP

inputs are limited around the midpoint of the physiological operating range [31].

In SHR, the ADN stimulation did not significantly affect the dynamic gain of the neural arc (Fig. 4, left), though mean of the gain plot showed a tendency of downward shift similar to that observed in WKY. The mean CSP was set at 160 mmHg, which is close to the midpoint of the sigmoidal nonlinearity between CSP and SNA in SHR [20]. As the standard deviation was set at 20 mmHg, CSP exceeded 190 mmHg in 6.7% of the time duration. In contrast to the case with WKY, however, these high CSP inputs silenced SNA in neither trial with or without the ADN stimulation (Fig. 3). There was a substantial margin for further sympathetic inhibition in SHR. Hence, it is likely that the ADN stimulation does not significantly affect the dynamic signal transduction from CSP to SNA via the mechanism of increasing the silencing period of SNA. The results are consistent with the static characteristics of the neural arc examined in a previous study, in which the percent minimum SNA attained by the maximum carotid sinus baroreflex activation is higher in SHR (approximately 30%) than in WKY (approximately 10%) [20].

A- and C-fiber baroreflex pathways have significant interactions as will be discussed in the next section. We therefore hypothesized that the C-fiber stimulation from the ADN would impede dynamic characteristics of the carotid sinus baroreflex. However, the tonic ADN stimulation did not affect the derivative characteristics of the neural arc as assessed by G_{slope} in WKY or SHR. The speed of AP response in the total baroreflex arc assessed by S_{slope}/S_{50} was unchanged between the trials with and without the ADN stimulation. Hence, the ADN stimulation reduced mean AP without changing the dynamic characteristics

of the carotid sinus baroreflex. In the present study, we used a GWN signal as an input for the CSP perturbation because it allows identification of linear dynamic characteristics even in the presence of significant noise contamination [18]. The GWN input is also robust against the presence of some type of nonlinearity in the system. As an example, if a given system is a cascade of a dynamic linear subsystem followed by a static nonlinear subsystem, the shape of the static nonlinear system alone does not affect the estimation of the overall system linear dynamics except for a factor of proportionality in theory [3]. While there is room for argument whether the results would be the same for different types of input signals, the GWN input may be the most rigorous test of the system dynamic characteristics.

Differences in A- and C-fiber baroreceptor pathways

There are distinct differences in A-fiber and C-fiber baroreflex pathways. C-fiber axons require higher voltage for activation compared with A-fiber axons. In addition, the C-fiber pathway can induce hypotensive effect at a frequency as low as 1 Hz, but the A-fiber pathway does not significantly contribute to hypotension in the frequency range less than 10 Hz [8]. Considering the large proportion of C-fiber axons (80–90%) in the ADN [1, 9], it may be argued that the frequency required for the hypotensive effect is merely the reflection of the total number of axonal discharge per time, i.e., ten-times higher frequency would be required for the A-fiber pathway compared with the C-fiber pathway to evoke the comparable hypotensive effect. According to the study by Fan et al. [8], however, the hypotensive effect induced by C-fiber stimulation alone reaches the plateau at approximately 10 Hz, and increasing the frequency of C-fiber stimulation

above 10 Hz does not further decrease AP. In contrast, the simultaneous A-and C-fiber stimulation can induce further depression of AP between 50 and 200 Hz, suggesting that the contribution of the A-fiber pathway cannot be explained by merely the total number of axonal discharge per time. The maximal hypotensive effect attained by A and C fiber stimulation was, however, modestly greater than the maximal hypotensive effect attained by the selective stimulation of the either fiber type, indicating the presence of an occlusive summation in the hypotensive effects between the A- and C-fiber pathways [8].

As mentioned in the introduction section, derivative characteristics of the neural arc, i.e., increasing dynamic gain with frequency, such as those shown in the left panels of Figures 1 and 3, are important for the baroreflex-mediated short-term AP regulation [10]. Although the derivative characteristics are partly ascribed to the dynamic transduction properties of the baroreceptors [16, 22], the central pathway from baroreceptor afferent signal to efferent SNA also contributes to the generation of the derivative characteristics. In a previous study, the A-fiber central pathway reveals stronger derivative characteristics than the C-fiber central pathway [28]. Conversely, the C-fiber pathway contributes more to sustained decreases in SNA and AP than the A-fiber pathway. The relative contribution of A- and C-fiber pathways should differ depending on the level of baroreceptor input pressure because C-fiber baroreceptors have high threshold and low firing frequency characteristics compared with A-fiber baroreceptors [24]. Near the midpoint pressure of the sigmoid curve of the neural arc, i.e., around the normal operating pressure, A-fiber baroreceptors are capable of regulating AP in the absence of C-fiber contribution, at least in the time window of 10 min

[27]. In the present study, high CSP inputs above the normal operating pressure occurred during the GWN-based pressure perturbation; and therefore, both A- and C-fiber baroreceptors probably contribute to the generation of the dynamic characteristics of the carotid sinus baroreflex neural arc. Hence, not only the interaction between A-fiber (carotid sinus) and C-fiber (ADN stimulation) but also the interaction between C-fiber (carotid sinus) and C-fiber (ADN stimulation) need to be considered to interpret the observed changes in the neural arc transfer function.

Limitations

First, because we performed the experiment under anesthetized rats, the results are not directly extendable to human hypertension. Moreover, we examined dynamic characteristics of the carotid sinus baroreflex while electrically stimulating the sectioned ADN, which is different from clinical CSS where the carotid sinus baroreflex is electrically activated while the aortic baroreceptors receive AP inputs. Nevertheless, we think the study design helped comprehensive understanding of interactions between the two baroreflex systems.

Second, the hypotensive effect attained by the ADN stimulation was statistically significant but relatively small in magnitude. This may be because the perturbation with GWN alone has a significant hypotensive effect, as shown in a previous study [19]. When we analyzed previously obtained data, mean AP during the GWN input (the mean of 120 mmHg and the standard deviation of 20 mmHg) was significantly lower than that during a static input at 120 mmHg (95.2 ± 8.6 vs. 107.3 ± 11.6 mmHg, n = 8, P = 0.010). Such a hypotensive effect

induced by the GWN input might have partly masked the hypotensive effect attained by the ADN stimulation. In addition, ΔAP induced by the ADN stimulation showed a tendency of becoming less negative with time elapsed, though ΔSNA remained unchanged (Table 3). Untested mechanisms such as the reduction of pressure diuresis during prolonged hypotension might have contributed to the gradual recovery of mean AP.

Third, the effect of ADN stimulation was only examined in an acute experimental setting. Although a constant mode of stimulation was used in the present study, ΔSNA did not show apparent change over time in WKY or SHR (Table 3), probably owing to a preferential stimulation of C-fiber baroreceptors. When low intensity stimulation is used, a bust mode of stimulation may increase the hypotensive effect induced by ADN stimulation [8]. Further study is required to identify the long-term effect of the ADN stimulation on dynamic characteristics of the carotid sinus baroreflex.

Finally, the vagi were sectioned to allow open-loop analysis of the carotid sinus baroreflex. As a result, the effect of the ADN stimulation on any cardiovascular control through the vagal system was not identified in the present study.

Perspective and significance

Although the role of the arterial baroreflex system in long-term AP control has been somewhat disregarded, recent clinical trials demonstrate that CSS can exert a long-term antihypertensive effect in patients with drug-resistant hypertension. The present results indicate that the tonic ADN stimulation does not significantly modify the dynamic characteristics of the carotid baroreflex.

Hence, an impact of the interaction between stimulated and unstimulated arterial baroreflexes during CSS on the normal short-term baroreflex regulation of AP is not likely to be large. In other words, the normal short-term baroreflex regulation of AP is likely preserved during CSS in hypertensive patients. In the present study, it was examined whether the electrical stimulation from one baroreflex system impedes normal short-term AP regulation from another unstimulated baroreflex system. When electrically activating the arterial baroreflex, there could be interactions within the stimulated baroreflex system. In CSS, the carotid sinus afferent fibers would be activated by both native pressure inputs and electrical stimulation. Future research is required to uncover the interactions within the stimulated baroreflex system. Understanding the interactions between native pressure inputs and electrical stimulation in activating the arterial baroreflex system may help identify reasons why there are responders and non-responders to CSS.

Sources of Funding

This study was partly supported by the Grant-in-Aid for Scientific Research (JSPS KAKENHI Grant Number 26750153, 15K09110, 15H03101), by Intramural Research Fund (26-6-24) for Cardiovascular Diseases of National Cerebral and Cardiovascular Center, and by the Takeda Medical Research Foundation.

Conflicts of Interest/Disclosures

The authors have no conflicts of interest or disclosures.

References

1. Andresen MC, Krauhs JM, Brown AM. Relationship of aortic wall and baroreceptor properties during development in normotensive and spontaneously hypertensive rats. Circ Res 43: 728–738, 1978.
2. Bakris GL, Nadim MK, Haller H, Lovett EG, Schafer JE, Bisognano JD. Baroreflex activation therapy provides durable benefit in patients with resistant hypertension: results of long-term follow-up in the Rheos Pivotal Trial. J Am Soc Hypertens 6: 152–158, 2012.
3. Bendat JS. Nonlinear system analysis and identification from random data. John Wiley & Sons, New York, 1990; pp 23–32.
4. Bendat JS, Piersol AG. Random Data. Analysis and Measurement Procedures. 4th edn. John Wiley & Sons, New Jersey, 2010; pp 173–199.
5. Braunwald E, Epstein SE, Glick G, Wechsler AS, Braunwald NS. Relief of angina pectoris by electrical stimulation of the carotid-sinus nerves. N Eng J Med 40: 269–276, 1969.
6. Chapleau MW, Hajduczok G, Abboud FM. Peripheral and central mechanisms of baroreflex resetting. Clin Exp Pharmacol Physiol Suppl 15: 31–43, 1989.
7. Cowley AW Jr, Liard JF, Guyton AC. Role of baroreceptor reflex in daily control of arterial blood pressure and other variables in dogs. Circ Res 32: 564–576, 1973.
8. Fan W, Schild JH, Andresen MC. Graded and dynamic reflex summation of myelinated and unmyelinated rat aortic baroreceptors. Am J Physiol 277: R748–R756, 1999.

9. Fazan VP, Salgado HC, Barreira AA. Aortic depressor nerve unmyelinated fibers in spontaneously hypertensive rats. Am J Physiol Heart Circ Physiol 280: H1560–H1564, 2001.
10. Ikeda Y, Kawada T, Sugimachi M, Kawaguchi O, Shishido T, Sato T, Miyano H, Matsuura W, Alexander J Jr, Sunagawa K. Neural arc of baroreflex optimizes dynamic pressure regulation in achieving both stability and quickness. Am J Physiol 271: H882–H890, 1996.
11. Iliescu R, Tudorancea I, Irwin ED, Lohmeier TE. Chronic baroreflex activation restores spontaneous baroreflex control and variability of heart rate in obesity-induced hypertension. Am J Physiol Heart Circ Physiol 305: H1080–H1088, 2013.
12. Kawada T, Li M, Kamiya A, Shimizu S, Uemura K, Yamamoto H, Sugimachi M. Open-loop dynamic and static characteristics of the carotid sinus baroreflex in rats with chronic heart failure after myocardial infarction. J Physiol Sci 60: 283–298, 2010.
13. Kawada T, Shimizu S, Kamiya A, Sata Y, Uemura K, Sugimachi M. Dynamic characteristics of baroreflex neural and peripheral arcs are preserved in spontaneously hypertensive rats. Am J Physiol Regul Integr Comp Physiol 300: R155–R165, 2011.
14. Kawada T, Sugimachi M. Open-loop static and dynamic characteristics of the arterial baroreflex system in rabbits and rats. J Physiol Sci 66: 15–41, 2016.
15. Kawada T, Uemura K, Kashihara K, Kamiya A, Sugimachi M, Sunagawa K. A derivative-sigmoidal model reproduces operating point-dependent

baroreflex neural arc transfer characteristics. Am J Physiol Heart Circ Physiol 286: H2272–H2279, 2004.

16. Kawada T, Yamamoto K, Kamiya A, Ariumi H, Michikami D, Shishido T, Sunagawa K, Sugimachi M. Dynamic characteristics of carotid sinus pressure–nerve activity transduction in rabbits. Jpn J Physiol 55: 157–163, 2005.
17. Lohmeier TE, Iliescu R, Dwyer TM, Irwin ED, Cates AW, Rossing MA. Sustained suppression of sympathetic activity and arterial pressure during chronic activation of the carotid baroreflex. Am J Physiol Heart Circ Physiol 299: H402–H409, 2010.
18. Marmarelis PZ, Marmarelis VZ. The white noise method in system indentification. In: Analysis of Physiological Systems. The White-Noise Approach. New York: Plenum, 1978, pp. 131–180.
19. Moslehpour M, Kawada T, Sunagawa K, Sugimachi M, Mukkamala R. Nonlinear identification of the total baroreflex arc: higher-order nonlinearity. Am J Physiol Regul Integr Comp Physiol 311: R994–R1003, 2016.
20. Sata Y, Kawada T, Shimizu S, Kamiya A, Akiyama T, Sugimachi M. Predominant role of neural arc in sympathetic baroreflex resetting of spontaneously hypertensive rats. Circ J 79: 592–599, 2015.
21. Sato T, Kawada T, Miyano H, Shishido T, Inagaki M, Yoshimura R, Tatewaki T, Sugimachi M, Alexander J Jr, Sunagawa K. New simple methods for isolating baroreceptor regions of carotid sinus and aortic depressor nerves in rats. Am J Physiol 276: H326–H332, 1999.
22. Sato T, Kawada T, Shishido T, Miyano H, Inagaki M, Miyashita H, Sugimachi

M, Knuepfer MM, Sunagawa K. Dynamic transduction properties of in situ baroreceptors of rabbit aortic depressor nerve. Am J Physiol 274: H358–H365, 1998.

23. Shoukas AA, Callahan CA, Lash JM, Haase EB. New technique to completely isolate carotid sinus baroreceptor regions in rats. Am J Physiol 260: H300–H303, 1991.
24. Thoren P, Munch PA, Brown AM. Mechanisms for activation of aortic baroreceptor C-fibres in rabbits and rats. Acta Physiol Scand 166: 167–174, 1999.
25. Thrasher TN. Unloading arterial baroreceptors causes neurogenic hypertension. Am J Physiol Regul Integr Comp Physiol 282: R1044–R1053, 2002.
26. Turner MJ, Kawada T, Shimizu S, Fukumitsu M, Sugimachi M. Differences in the dynamic baroreflex characteristics of unmyelinated and myelinated central pathways are less evident in spontaneously hypertensive rats. Am J Physiol Regul Integr Comp Physiol 309: R1397–R1405, 2015.
27. Turner MJ, Kawada T, Shimizu S, Fukumitsu M, Sugimachi M. Open-loop characteristics of the arterial baroreflex after blockade of unmyelinated baroreceptors with resiniferatoxin. Auton Neurosci 193: 38–43, 2015.
28. Turner MJ, Kawada T, Shimizu S, Sugimachi M. Sustained reduction in blood pressure from electrical activation of the baroreflex is mediated via the central pathway of unmyelinated baroreceptors. Life Sci 106: 40–49, 2014.
29. Wallbach M, Lehnig LY, Schroer C, Lüders S, Böhning E, Müller GA, Wachter R, Koziolek MJ. Effects of baroreflex activation therapy on

598 ambulatory blood pressure in patients with resistant hypertension.
599 Hypertension 67: 701–709, 2016.
600 30. Yamamoto H, Kawada T, Shimizu S, Kamiya A, Turner MJ, Miyazaki S,
601 Sugimachi M. Acute effects of intravenous nifedipine or azelnidipine on
602 open-loop baroreflex static characteristics in rats. Life Sci 126: 37–41, 2015.
603 31. Yamazaki T, Sagawa K. Summation of sinoaortic baroreflexes depends on
604 size of input signals. Am J Physiol 257: H465–H472, 1989.
605

606 Table 1. Parameters of carotid sinus baroreflex dynamic characteristics in
607 Wistar–Kyoto (WKY) rats.

	WKY Control	WKY ADNS	P value
Neural arc			
$G_{0.01}$, au/mmHg	1.038 ± 0.043	0.827 ± 0.111	0.141
$G_{0.1}$, au/mmHg	1.288 ± 0.093	0.911 ± 0.057	0.006
G_{1}, au/mmHg	4.245 ± 0.237	3.332 ± 0.298	0.004
G_{slope}, dB/decade	12.55 ± 0.93	13.03 ± 1.28	0.542
S_{peak}, au/mmHg	–2.982 ± 0.126	–2.424 ± 0.156	0.034
T_{peak}, s	0.450 ± 0.027	0.513 ± 0.035	0.140
S_{10}	–0.948 ± 0.035	–0.813 ± 0.079	0.116
Peripheral arc			
$G_{0.01}$, mmHg/au	0.429 ± 0.078	0.391 ± 0.084	0.323
$G_{0.1}$, mmHg/au	0.137 ± 0.026	0.118 ± 0.023	0.138
$G_{0.5}$, mmHg/au	0.013 ± 0.003	0.013 ± 0.003	0.995
G_{slope}, dB/decade	–31.30 ± 1.58	–33.00 ± 1.64	0.106
S_{slope}, mmHg·au^{-1}·s^{-1}	0.066 ± 0.011	0.058 ± 0.010	0.061
S_{50}, mmHg/au	0.459 ± 0.082	0.407 ± 0.088	0.084
S_{slope}/S_{50}, s^{-1}	0.144 ± 0.007	0.150 ± 0.007	0.456
Total reflex arc			
$G_{0.01}$, mmHg/mmHg	0.485 ± 0.091	0.380 ± 0.099	0.043
$G_{0.1}$, mmHg/mmHg	0.185 ± 0.035	0.112 ± 0.024	0.018
$G_{0.5}$, mmHg/mmHg	0.051 ± 0.010	0.038 ± 0.009	0.083
G_{slope}, dB/decade	–21.92 ± 1.66	–22.29 ± 1.49	0.753
S_{slope}, mmHg·mmHg^{-1}·s^{-1}	–0.106 ± 0.020	–0.069 ± 0.013	0.011
S_{50}, mmHg/mmHg	–0.505 ± 0.093	–0.398 ± 0.097	0.040
S_{slope}/S_{50}, s^{-1}	0.210 ± 0.023	0.193 ± 0.021	0.256

608 Values are mean ± SE (n = 8). ADNS: aortic depressor nerve stimulation. $G_{0.01}$,
609 $G_{0.1}$, $G_{0.5}$, and G_{1}: dynamic gain values at 0.01, 0.1, 0.5, and 1 Hz, respectively.
610 G_{slope}: slope of dynamic gain. S_{peak} and T_{peak}: negative peak response and time
611 to the negative peak in the neural arc step response. S_{10}: step response at 10 s.
612 S_{slope}: initial slope of the step response. S_{50}: step response at 50 s. S_{slope}/S_{50}: the
613 ratio of S_{slope} to S_{50}. P values were obtained by paired-t test.
614

Table 2. Parameters of carotid sinus baroreflex dynamic characteristics in spontaneously hypertensive rats (SHR).

	SHR Control	SHR ADNS	P value
Neural arc			
$G_{0.01}$, au/mmHg	0.937 ± 0.079	0.611 ± 0.148	0.107
$G_{0.1}$, au/mmHg	1.204 ± 0.263	0.889 ± 0.222	0.264
G_{1}, au/mmHg	6.654 ± 1.024	5.638 ± 0.698	0.360
G_{slope}, dB/decade	17.37 ± 1.01	17.47 ± 1.64	0.946
S_{peak}, au/mmHg	–3.968 ± 0.677	–3.191 ± 0.418	0.193
T_{peak}, s	0.357 ± 0.030	0.386 ± 0.026	0.172
S_{10}	–0.732 ± 0.113	–0.610 ± 0.135	0.438
Peripheral arc			
$G_{0.01}$, mmHg/au	0.463 ± 0.139	0.463 ± 0.133	0.998
$G_{0.1}$, mmHg/au	0.190 ± 0.069	0.175 ± 0.071	0.170
$G_{0.5}$, mmHg/au	0.022 ± 0.008	0.024 ± 0.008	0.606
G_{slope}, dB/decade	–23.98 ± 1.43	–24.80 ± 1.80	0.624
S_{slope}, mmHg·au^{-1}·s^{-1}	0.086 ± 0.030	0.077 ± 0.026	0.113
S_{50}, mmHg/au	0.448 ± 0.134	0.457 ± 0.130	0.767
S_{slope}/S_{50}, s^{-1}	0.178 ± 0.020	0.161 ± 0.029	0.245
Total reflex arc			
$G_{0.01}$, mmHg/mmHg	0.447 ± 0.095	0.364 ± 0.082	0.319
$G_{0.1}$, mmHg/mmHg	0.216 ± 0.048	0.178 ± 0.059	0.369
$G_{0.5}$, mmHg/mmHg	0.097 ± 0.029	0.102 ± 0.041	0.804
G_{slope}, dB/decade	–12.99 ± 1.50	–10.52 ± 2.69	0.502
S_{slope}, mmHg·mmHg^{-1}·s^{-1}	–0.157 ± 0.035	–0.115 ± 0.036	0.030
S_{50}, mmHg/mmHg	–0.437 ± 0.099	–0.286 ± 0.094	0.150
S_{slope}/S_{50}, s^{-1}	0.367 ± 0.048	0.516 ± 0.225	0.514

Values are mean ± SE (n = 7). ADNS: aortic depressor nerve stimulation. $G_{0.01}$, $G_{0.1}$, $G_{0.5}$, and G_{1}: dynamic gain values at 0.01, 0.1, 0.5, and 1 Hz, respectively. G_{slope}: slope of dynamic gain. S_{peak} and T_{peak}: negative peak response and time to the negative peak in the neural arc step response. S_{10}: step response at 10 s. S_{slope}: initial slope of the step response. S_{50}: step response at 50 s. S_{slope}/S_{50}: the ratio of S_{slope} to S_{50}. P values were obtained by paired-t test.

Table 3. Time dependent changes in mean arterial pressure (AP) and sympathetic nerve activity (SNA) during Gaussian white noise inputs.

	bin #1 (0–5 min)	bin #2 (5–10 min)	bin #3 (10–15 min)	bin #4 (15–20 min)
WKY (n = 8)				
Mean AP without ADNS, mmHg	87.4 ± 8.4	91.8 ± 7.8	89.7 ± 6.3	89.6 ± 6.5
ΔAP by ADNS, mmHg	–21.4 ± 5.5	–14.6 ± 2.5	–6.6 ± 3.6	–11.4 ± 5.1
Mean SNA without ADNS, a.u.	59.8 ± 12.2	72.5 ± 14.5	72.4 ± 14.0	79.4 ± 14.0 **
ΔSNA by ADNS, a.u.	–27.3 ± 4.4	–30.0 ± 3.7	–19.4 ± 8.3	–25.2 ± 9.8
SHR (n = 7)				
Mean AP without ADNS, mmHg	129.7 ± 14.3	130.3 ± 11.4	132.4 ± 10.5	128.5 ± 11.2
ΔAP by ADNS, mmHg	–37.5 ± 10.1	–17.9 ± 7.0	–19.8 ± 4.3	–8.0 ± 5.8 *
Mean SNA without ADNS, a.u.	225.0 ± 30.3	244.3 ± 32.3	259.2 ± 38.0 **	260.2 ± 39.2 **
ΔSNA by ADNS, a.u.	–75.7 ± 22.1	–72.6 ± 24.0	–76.4 ± 23.4	–64.7 ± 21.7

Values are mean ± SE. Data were obtained from Wistar–Kyoto (WKY) and spontaneously hypertensive rats (SHR). AP: arterial pressure, SNA: sympathetic nerve activity, ADNS: aortic depressor nerve stimulation. a.u.: arbitrary units. ΔAP and ΔSNA indicate the differences in mean AP and mean SNA between trials with and without ADNS. *P < 0.05 and **P < 0.01 against the value in bin #1 by repeated-measures analysis of variance followed by the Dunnett's test.

Figure legends

Figure 1.

Typical time series obtained from a Wistar–Kyoto rat. Carotid sinus pressure (CSP) was perturbed according to a Gaussian white noise signal with a mean of 120 mmHg with (middle panels) or without (left panels) the aortic depressor nerve (ADN) stimulation. The arterial pressure (AP) signals are displayed as 200-Hz sampled signals (gray lines) and 2-s moving averaged signals (black lines). The sympathetic nerve activity (SNA) signals are displayed as 10-Hz resampled signals (gray lines) and 2-s moving averaged signals (black lines). The ADN stimulation lowered mean AP and SNA. Unloading of CSP at the end of the experiment increased mean AP and SNA (right panels). Administration of hexamethonium bromide (C6) decreased SNA to the noise level.

Figure 2.

Transfer functions (upper panels) and step responses (bottom panels) relating to the neural arc (left panels), peripheral arc (middle panels), and total reflex arc (right panels) obtained in Wistar–Kyoto rats. Gray lines indicate the trial without the aortic depressor nerve (ADN) stimulation, and black lines indicate the trial with the ADN stimulation. The ADN stimulation slightly moved the dynamic gain of the neural arc transfer function downward, but it did not significantly affect the derivative characteristics. The lines are mean ± SE (n = 8).

Figure 3.

Typical time series obtained from a spontaneously hypertensive rat. Carotid

654 sinus pressure (CSP) was perturbed according to a Gaussian white noise signal
655 with a mean of 160 mmHg with (middle panels) or without (left panels) the aortic
656 depressor nerve (ADN) stimulation. The arterial pressure (AP) signals are
657 displayed as 200-Hz sampled signals (gray lines) and 2-s moving averaged
658 signals (black lines). The sympathetic nerve activity (SNA) signals are displayed
659 as 10-Hz resampled signals (gray lines) and 2-s moving averaged signals (black
660 lines). The ADN stimulation lowered mean AP and SNA, but there was a
661 significant margin for further SNA suppression. Unloading of CSP at the end of
662 the experiment increased mean AP and SNA (right panels). Administration of
663 hexamethonium bromide (C6) decreased SNA to the noise level.
664
665 Figure 4.
666 Transfer functions (upper panels) and step responses (bottom panels) relating to
667 the neural arc (left panels), peripheral arc (middle panels), and total reflex arc
668 (right panels) obtained in spontaneously hypertensive rats. Gray lines indicate
669 the trial without the aortic depressor nerve (ADN) stimulation, and black lines
670 indicate the trial with the ADN stimulation. Although the ADN stimulation tended
671 to move the dynamic gain of the neural arc transfer function downward, these
672 changes were not statistically significant. The derivative characteristics of the
673 neural arc were not significantly affected by the ADN stimulation. The lines are
674 mean ± SE (n = 7).

Figure 1

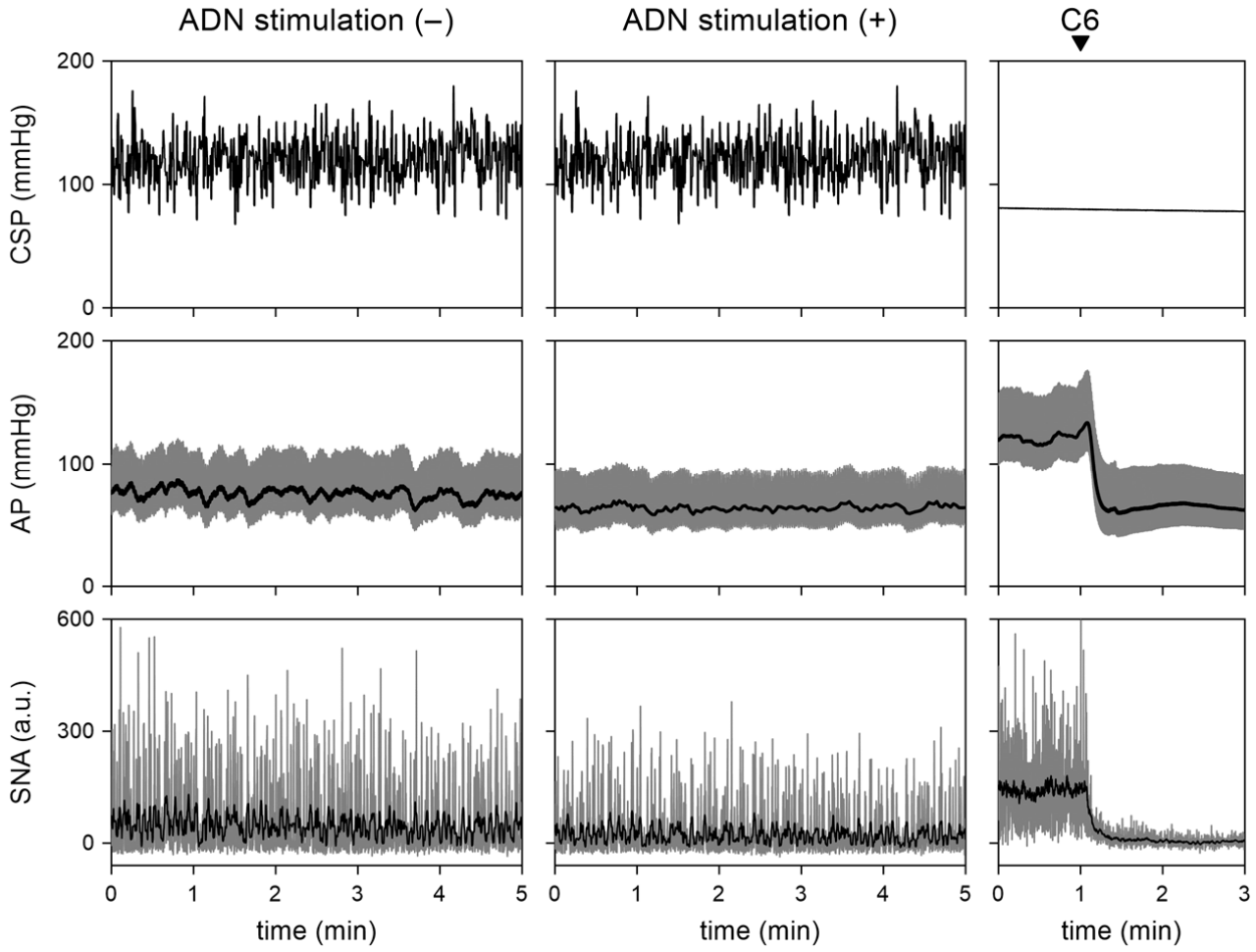
ADN stimulation (–)
ADN stimulation (+)
C6
CSP (mmHg)
AP (mmHg)
SNA (a.u.)
200
100
0
600
300
0
1
2
3
4
5
time (min)

Figure 2

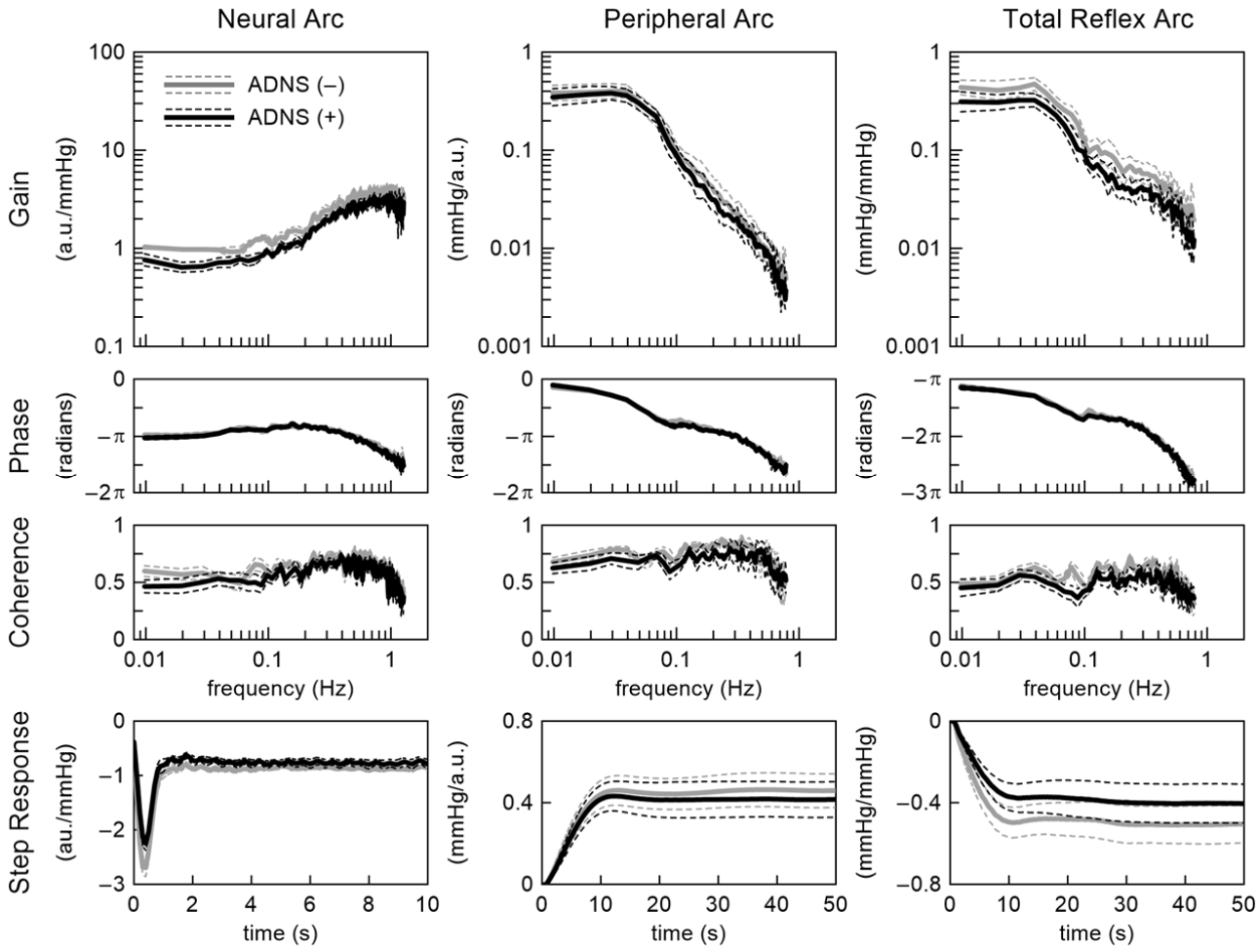
Neural Arc
Peripheral Arc
Total Reflex Arc
ADNS (–)
ADNS (+)
Gain
(a.u./mmHg)
(mmHg/a.u.)
(mmHg/mmHg)
Phase
(radians)
Coherence
frequency (Hz)
Step Response
(au./mmHg)
time (s)

Figure 3

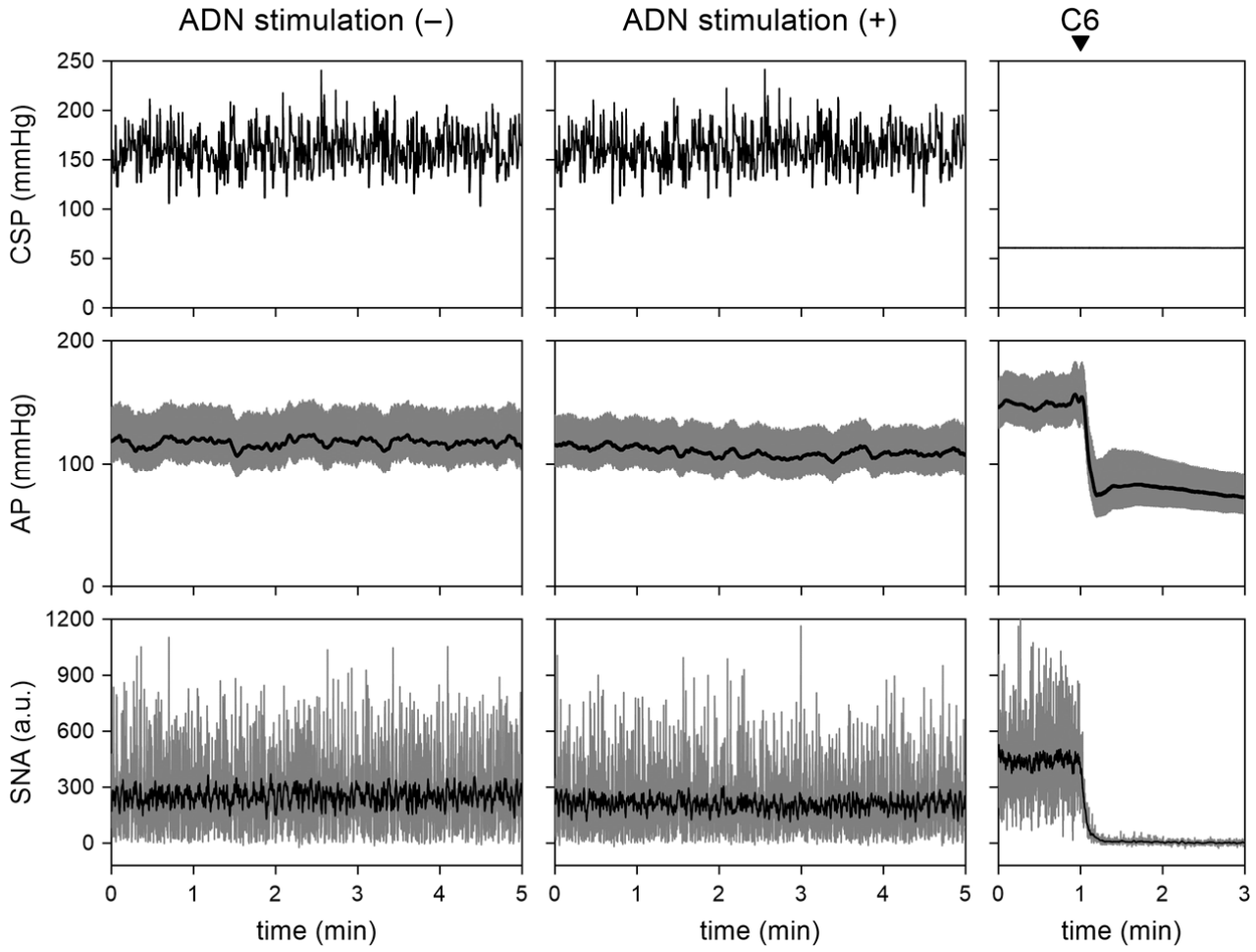
ADN stimulation (–)
ADN stimulation (+)
C6
CSP (mmHg)
AP (mmHg)
SNA (a.u.)
time (min)
time (min)
time (min)

Figure 4

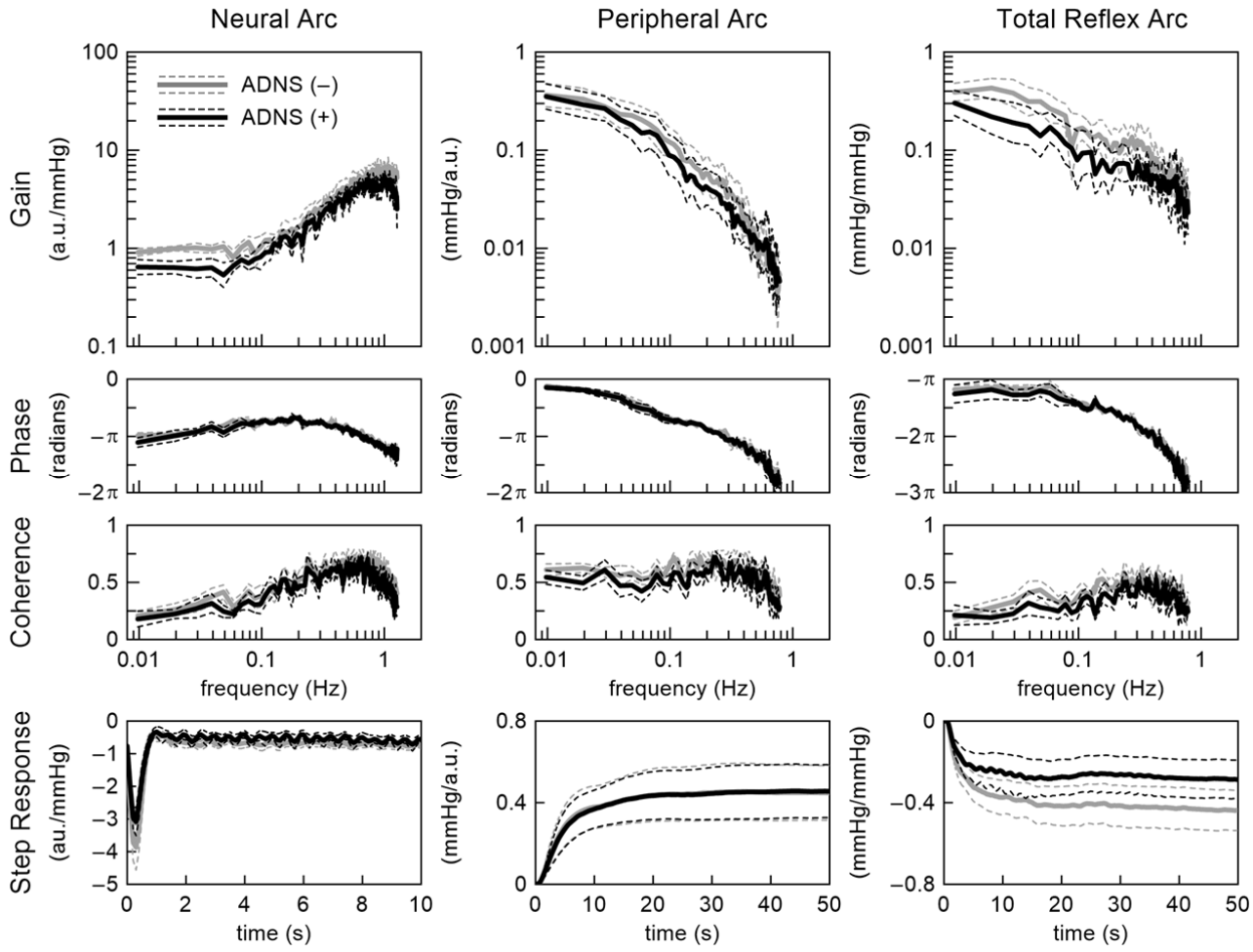
Neural Arc
Peripheral Arc
Total Reflex Arc
ADNS (–)
ADNS (+)
Gain
(a.u./mmHg)
(mmHg/a.u.)
(mmHg/mmHg)
Phase
(radians)
Coherence
frequency (Hz)
Step Response
(au./mmHg)
time (s)